The Three-Dimensional Boundary Layer on a Rotating Flat Plate as Influenced by the Containing End-Walls

H. Ekerol* and J. W. Railly†

Growth of the turbulent boundary layer over a flat plate rotating about an axis parallel to the leading edge is considered in which the axial length (or span) is contained between rotating radial end-plates (the hub and shroud, in effect, of a centrifugal impeller). The problem of the influence of the cross-flows in the boundary layers on the end-plates as they affect the blade boundary layer is considered. The latter is treated as a three-dimensional problem and the dependence of the solution on the boundary conditions is discussed. The integral equations of this boundary layer reduce to a pair of quasi-linear partial differential equations which are weakly elliptic, parabolic, or weakly hyperbolic according to the rotation number. When the equations are exactly parabolic and the boundary layers remain thin it is shown that the end-plate boundary layers can have no influence upon the blade boundary layer if the flow is initially radial; separation of the end-plate cross flows takes place in the corners.

NOTATION

A, B, C, D, E	constants as defined in eq. (6)
A_1, A_2, etc.	constants as defined in eq. (11)
b	semi-span of blade
C_f	skin friction coefficient
F	integral quantity, eq. (6)
G, g	functions defined in eqs. (7) and (8)
n	power law, eq. (7)
p	pressure
r, s	defined in eq. (13)
U_1	free stream velocity
u, v, w	boundary layer velocities along x, y, z
x, y, z	co-ordinate directions, see Fig. 2
α	along characteristic
δ	boundary layer thickness
δ_x^*	x-wise displacement thickness
θ	momentum thickness, eq. (6)
η	ratio y/δ
ν	kinematic viscosity
ρ	density
τ_w	wall-shear stress
Ω	angular velocity of rotor

Subscripts

b	blade boundary layer
w	end-wall boundary layer

INTRODUCTION

In a paper by Moore (**1**), a model was put forward for the behaviour of the flow in a corner, applicable, for example, to the corner between the blade of a radial impeller and the end-wall (shroud or hub). This model, which may be termed the 'corner-flow model' makes the assumption that if there is a boundary layer flow on the end-wall which has a component into (or out of) the corner (by virtue of the presence of a boundary layer deflection angle on the end-wall) then the flow corresponding to this angle is accepted by the blade boundary layer and determines one of the boundary conditions. This situation is shown in Fig. 1 where the two boundary layers meet at the corner and where δ_w and δ are, respectively, the thicknesses of the end-wall layer and blade layer. Making use of this model, Sharma and Railly (**2**) presented a simple calculation of the three-dimensional influence of the end-wall boundary layer on the blade boundary layer of a radial impeller at the central span position, Fig. 2. The corner-flow model gave the simple result in the corner at $z = 0$

$$\varepsilon(0) = \varepsilon_w \delta_w / \delta \tag{1}$$

where ε, ε_w are the blade and end-wall boundary layer deflection angles, assuming similar power law profiles.

The observation was then made that the three-dimensional influence on the equations at the centre-plane (a plane-of-symmetry) was confined to the term $\partial w/\partial z$ appearing in the equation of continuity, where w is the spanwise (the z-direction) component. Making the assumption that this gradient was uniform with z then w could be given by the relation

$$w = \varepsilon_b (z/b) g(\eta) G(\eta) U_1 \tag{2}$$

where the functions g, G of η are the functions controlling the cross-flow and mainstream flow velocity profiles of the blade boundary layer. The resulting blade boundary layer equation was solved at the centre-plane (using the Moses strip—integral method) and predictions of the turbulent layer (as affected by the end-wall) were made; the solutions as given in that paper were, however, not numerically accurate and need to be revised.

However, difficulties arose when it was decided not to confine the solution to the centre-plane but to investigate possible solutions of the three-dimensional boundary layer over the blade as affected by the end-wall condition. The following analysis is concerned with that situation.

Received 13 July 1979 and accepted for publication on 19 December 1979.

* Research Fellow, University of Birmingham.
† Professor of Turbomachinery, University of Birmingham.

0142/727X/80/0300-0035$02.00 © MEP Ltd 1980

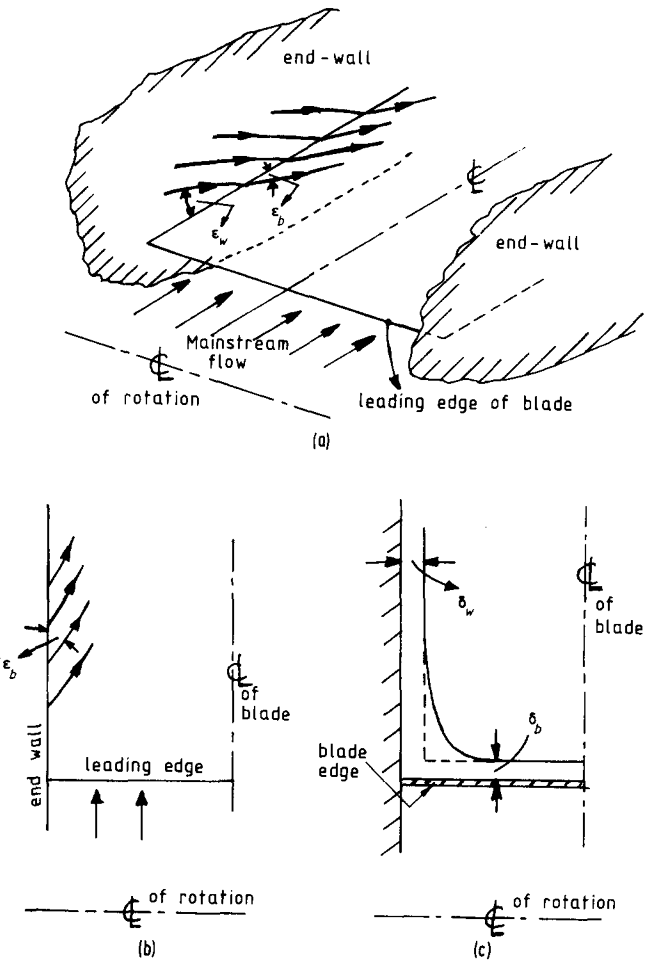

Fig. 1. (a) View of blade and locus of wall stress on blade and end-wall. (b) Plan of blade. (c) Corner-flow model looking in flow direction

DEVELOPMENT OF THE EQUATIONS FOR THE THREE-DIMENSIONAL BLADE BOUNDARY LAYER

Integration over the boundary layer thickness of the equations of motion produces a pair of momentum integral equations in terms of the independent variables x and z (see Fig. 2). These are thus a pair of partial differential equations involving the first order derivatives of various integral thicknesses. A more detailed discussion of the analysis is given by Ekerol (3) and only the equations which resulted need be quoted here; see also Appendix 1. They are

$$\frac{\partial \theta_{xx}}{\partial x}+\left(\frac{U_1'}{U_1}\right)(2\theta_{xx}+\delta_x^*)+\frac{\partial \theta_{xz}}{\partial z} = \frac{\tau_{wx}}{\rho U_1^2}+R_0\left\{\frac{U_1'}{U_1}(\delta-\delta_x^*)+\frac{\partial}{\partial x}(\delta-\delta_x^*) + \frac{\partial}{\partial z}\int_0^\delta \int_0^y \frac{w}{U_1}\,\mathrm{d}y\,\mathrm{d}y\right\} \quad (3)$$

$$\frac{\partial \theta_{zx}}{\partial x}+\frac{\partial \theta_{zz}}{\partial z}=\frac{\tau_{wz}}{\rho U_1^2} \quad (4)$$

The second term on the r.h.s. of eq. (3) represents the influence of rotation through the rotation number,

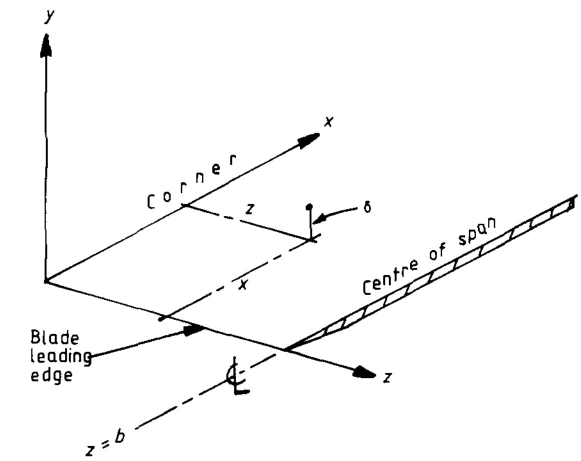

Fig. 2. Co-ordinate system for blade boundary layer, δ is blade boundary layer thickness

$R_0=(2\Omega\delta/U_1)$. The momentum thicknesses are as follows

$$\begin{aligned}
\theta_{xx}&=\left(\frac{1}{U_1^2}\right)\int_0^\delta u(U_1-u)\,\mathrm{d}y\\
\theta_{xz}&=\left(\frac{1}{U_1^2}\right)\int_0^\delta w(U_1-u)\,\mathrm{d}y\\
\theta_{zx}&=-\left(\frac{1}{U_1^2}\right)\int_0^\delta uw\,\mathrm{d}y\\
\theta_{zz}&=-\left(\frac{1}{U_1^2}\right)\int_0^\delta w^2\,\mathrm{d}y
\end{aligned} \quad (5)$$

and the prime in eqs. (3) and (4) denotes differentiation with respect to x.

Equation (3) is similar to that given by Moore (loc. cit.) in his analysis of the boundary layer in a rotating, radial channel, rectangular in cross-section. However, it differs from his equation by virtue of the second term in the brackets on the right. The reason for this arises from his neglect of the term $U(\partial\delta/\partial x)$ appearing after differentiation of the second equation of motion (Appendix 1).

Equations (3) and (4) may be simplified on the basis of eq. (2a), see below, so that the number of dependent variables may be reduced to two, namely, ε and δ. In fact the various thicknesses may be written in terms of G and g as follows

$$\begin{aligned}
\theta_{xx}&=\delta\int_0^1 G(1-G)\,\mathrm{d}\eta=A\delta\\
\delta_x^*&=\delta\int_0^1 (1-G)\,\mathrm{d}\eta=B\delta\\
\theta_{xy}&=\varepsilon\delta\int_0^1 Gg(1-G)\,\mathrm{d}\eta=C\varepsilon\delta\\
\theta_{zx}&=-\varepsilon\delta\int_0^1 G^2g\,\mathrm{d}\eta=D\varepsilon\delta\\
\theta_{zz}&=-\varepsilon^2\delta\int_0^1 G^2g^2\,\mathrm{d}\eta=E\varepsilon^2\delta
\end{aligned} \quad (6)$$

$$\int_0^\delta\int_0^y \frac{w}{U_1}\,\mathrm{d}y\,\mathrm{d}y=\varepsilon\delta^2\int_0^1\int_0^\eta Gg\,\mathrm{d}\eta=F\varepsilon\delta^2$$

in which the last of these appears in eq. (3). The function G represents the 'streamwise' profile, u/U_1. For simplicity a power law is used for G and the Prandtl–Mager law for g. Introducing exponent, n, these functions may be given by

$$G = \eta^{1/n} \quad (7)$$

and

$$g = (1 - \eta)^2 \quad (8)$$

so that the velocity component, w, is given by

$$w = \varepsilon g(\eta)G(\eta) \quad (2a)$$

The evaluation of all of eqs. (6) in terms of (7) and (8) is easily carried out, the coefficients A to F all being simple functions of n.

In terms of these and the other parameters, eqs. (3) and (4) become

$$(A - JR_0)\delta_x + (C - 2FR_0)\varepsilon\delta_z + (C - FR_0)\delta\varepsilon_z = \frac{C_f}{2} + \delta(JR_0 - 2A - B)\frac{U_1'}{U_1} \quad (9)$$

$$D\varepsilon\delta_x + E\varepsilon^2\delta_z + D\delta\varepsilon_x + 2E\varepsilon\delta\varepsilon_z = \varepsilon C_f/2 \quad (10)$$

in which the subscripts denote partial differentiation as appropriate and J is $1 - B$.

It is convenient to replace these equations with another set in terms of coefficients A_1 to E_1, A_2 to E_2, as follows

$$\begin{aligned} A_1 &= A - JR_0 \\ B_1 &= (C - 2FR_0)\varepsilon \\ C_1 &= 0 \\ D_1 &= (C - FR_0)\delta \\ E_1 &= -C_f/2 - (JR_0 - 2A - B)(U_1'/U_1)\delta \\ A_2 &= D\varepsilon \\ B_2 &= E\varepsilon^2 \\ C_2 &= D\delta \\ D_2 &= 2E\varepsilon\delta \\ E_2 &= -\varepsilon C_f/2 \end{aligned} \quad (11)$$

DISCUSSION OF THE EQUATIONS

Equations (9) and (10) may now be written

$$A_1\delta_x + B_1\delta_z + C_1\varepsilon_x + D_1\varepsilon_z + E_1 = 0 \quad (9a)$$

$$A_2\delta_x + B_2\delta_z + C_2\varepsilon_x + D_2\varepsilon_z + E_2 = 0 \quad (10a)$$

and are seen to be quasi-linear in the x, z derivatives of δ and ε.

Initially, various attempts to solve these equations numerically starting with the specification of δ and ε along $z = 0$ (the x-axis) and δ = constant and $\varepsilon = 0$ along the leading edge, $x = x_i$, failed to produce a solution thus questioning the freedom to choose δ, ε in this way at the leading edge. However, it was felt, in principle, that δ and ε could be so chosen because the flow meeting the leading edge, would necessarily be parallel to the x-axis making ε equal to zero. Equations (9a) and (10a) were next examined to ascertain their type, by testing the coefficients of the derivatives for the existence of characteristics. The procedure for the treatment of a pair of quasi-linear partial differential equations for two dependent and two independent variables has been described by Courant and Friedrichs (**4**) and the treatment below is similar. The existence or otherwise of characteristic depends on the sign of the determinant, Δ, given by

$$\Delta = b_0^2 - a_0c_0 \quad (12)$$

where

$$\begin{aligned} a_0 &= A_1C_2 - A_2C_1 \\ 2b_0 &= A_1D_2 - A_2D_1 + B_1C_2 - B_2C_1 \\ c_0 &= B_1D_2 - B_2D_1 \end{aligned}$$

The equations of the characteristics, ζ^+, ζ^-, are then

$$\begin{aligned} \zeta^+ &= \varepsilon(b_0 + \sqrt{\Delta})/a_0 = \varepsilon r \\ \zeta^- &= \varepsilon(b_0 - \sqrt{\Delta})/a_0 = \varepsilon s \end{aligned} \quad (13)$$

The behaviour of this set of equations was studied in detail by Ekerol (loc. cit.) and the dependence of type upon rotation number, R_0, and power law exponent, n, was explored. The value of Δ had to be examined, numerically, quite accurately, since the value was always very small for the likely range of R_0 and n. The result of the calculation is given in Fig. 3 where it may be seen that the system of eqs. (3) and (4) could be either hyperbolic, parabolic, or elliptic. In fact the set was elliptic for rotation numbers in the range $-0{\cdot}04$ to $+0{\cdot}12$ depending slightly on the value of n. When this type of analysis was first carried out, only the case of R_0 equal to zero was considered and for all the values of n used the set was only just elliptic and the physical significance of this result was not clear. However, we are indebted to Professor Skyrme (**5**) for the following procedure. He took the view that the system would not behave significantly differently if it were assumed that the set was exactly parabolic, that is, Δ equal to zero (the computed value of Δ for R_0 zero and n equal to 7 being -2×10^{-6}). Referring to eqs. (9) and (10), for R_0 zero, the former is divided by A and the latter by D and re-arranged as follows

$$\left(\frac{\partial}{\partial x} + \frac{C}{A}\varepsilon\frac{\partial}{\partial z}\right)\delta + \frac{C}{A}\delta\frac{\partial\varepsilon}{\partial z} = \frac{C_f}{2A} - \left(2 + \frac{B}{A}\right)\frac{\partial}{U_1}U_1' \quad (9b)$$

$$\left(\frac{\partial}{\partial x} + \frac{E}{D}\varepsilon\frac{\partial}{\partial z}\right)\delta + \frac{\delta}{\varepsilon}\left(\frac{\partial}{\partial x} + 2\frac{E}{D}\varepsilon\frac{\partial}{\partial z}\right)\varepsilon = \left(\frac{C_f}{2D}\right) \quad (10b)$$

In view of the above statement, it is now permissible to write $C/A = E/D = P$ and the equations are now exactly parabolic (for $n = 7$, P is about $\frac{1}{2}$); this entailed a very slight adjustment to the values of the coefficients. The following result is obtained by subtracting eq. (10b) from (9b), namely

$$\left(\frac{\partial}{\partial x} + \frac{\varepsilon}{2}\frac{\partial}{\partial z}\right)\varepsilon = -\varepsilon\left(\frac{0{\cdot}021}{U_1^{0{\cdot}25}}\delta^{-1{\cdot}25} - 3{\cdot}25\frac{U_1'}{U_1}\right) \quad (14)$$

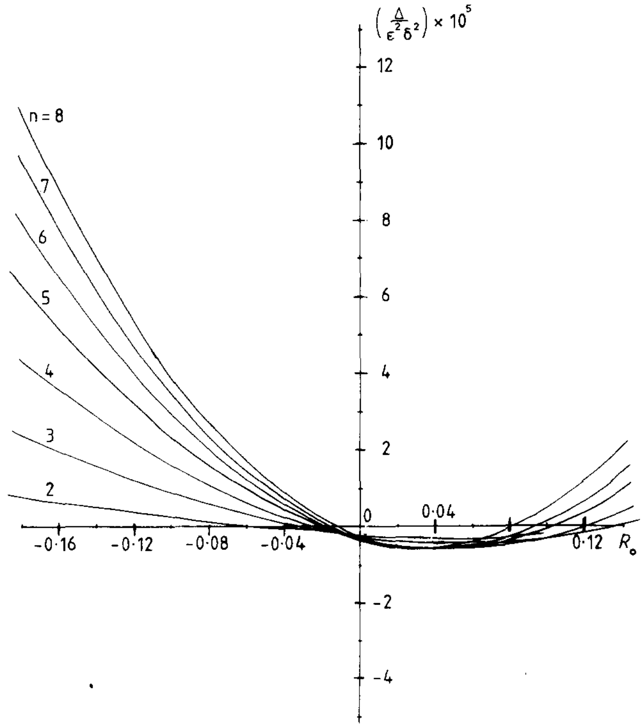

Fig. 3. Effect of rotation number, R_0, and index, n, upon Δ

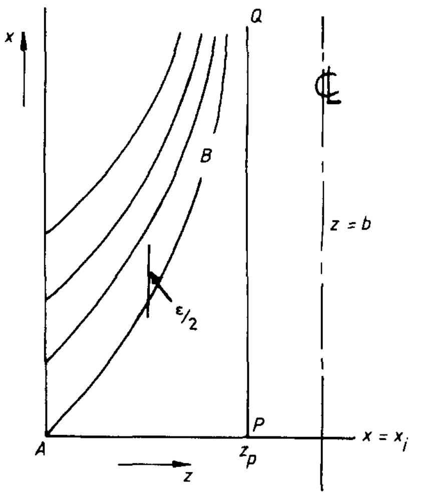

Fig. 4. Characteristics in x–z plane; AB, PQ limiting characteristics, ε zero for $z \geq z_p$; (plan view of blade surface which is coincident with x–z plane

in which the skin friction law

$$C_f/2 = 0{\cdot}0225/R_\delta^{0{\cdot}25}$$

has been used, with n being put equal to 7 and the kinematic viscosity for air, $1{\cdot}5 \times 10^{-5}$ m^2/s, inserted. The operator on the left of eq. (14) shows that the derivatives have combined to a single total derivative along a line such that

$$\mathrm{d}z/\mathrm{d}x = \varepsilon/2$$

Thus the lines of slope $\varepsilon/2$ are the characteristics in the x–z plane. That is to say, that the pair of equations (9) and (10) combine to form derivatives only in the direction of lines inclined to the x-axis by the angle $\varepsilon/2$ and, consequently, no information as to the behaviour of either variable to either side of that line can be obtained from the equations. Since gradient U_1' is frequently either zero or negative, which is the case on the suction side of the blade, then eq. (14) reveals that ε must decrease numerically along the characteristics, which therefore must approach some limiting line, say $z_p =$ constant, more or less quickly depending on the initial values of ε from $z = 0$ to $z = z_p$ provided $\varepsilon = 0$ for z greater than z_p; this situation is demonstrated in Fig. 4. Along the x-axis, it might be allowed that both variables, δ and ε, may be specified along that line (which is the corner between the blade and the end-wall) so that the resulting characteristics would appear as in Fig. 4. Since PQ is the limiting characteristic it is evident that a solution could be found in the portion of the x–z plane bounded by the x-axis, by AP and by PQ, (since values of δ and ε have been specified also along AP with the condition that ε decreases with z dropping to zero at the point P and thereafter). However, if the view be taken that an initial prescription along the line $x = x_i$ (such as the leading edge) of ε and δ is allowable, then the initial condition, $\varepsilon = 0$, is allowed and requires, as eq. (14) shows, that ε will remain zero for all $x > x_i$, or, in physical terms, that nowhere may the cross-flow emanating from the end-wall boundary layer penetrate the blade boundary layer. Conversely, if we assume that ε be not specified along $x = x_i$, (the z-axis), then boundary values of δ, ε along $z = 0$ (the x-axis) for x greater than x_i (see Fig. 4) are unable to affect any values of ε to the right of the limiting characteristic, AB, emanating from A and of slope $\varepsilon_A/2$ initially. Since the condition of symmetry, $\varepsilon = 0$, along the line $z = b$ is a required boundary condition in this problem, then the flow to the right of the region bounded by AB and the line $z = b$ may only be determined by values of ε and δ specified along $x = x_i$.

POSSIBLE SOLUTION PROCEDURE

The conclusion is drawn that a solution over the whole field, that is, for x greater than x_i and for z between zero and b may be obtained, provided δ and ε are specified along the z-axis from zero to b and up the x-axis for x greater than x_i. It will be necessary for ε values along the x-axis to be positive in this case for if they were negative the solution would be determined from the above portion of the z-axis.

Considering the characteristics emanating from the x-axis as shown in Fig. 4 then eq. (9b) may be solved numerically for δ along the characteristic direction for a short step, δx, δz after eq. (14) has been solved (in the same direction) for ε. Equation (9b) requires the gradient, $\partial\varepsilon/\partial z$, along the same characteristic and this follows from eq. (14) and the knowledge of ε along the x-axis.

Replacing $\partial\varepsilon/\partial z$, denoted by ε_z, in terms of the operator on the left of eq. (14), which is denoted by the subscript, α, as follows

$$\varepsilon_z = \left(\frac{2}{\varepsilon}\right)\left\{\left(\frac{\mathrm{d}\varepsilon}{\mathrm{d}x}\right)_\alpha - \varepsilon_x\right\} \qquad (14a)$$

then

$$\left(\frac{d\delta}{dx}\right)_\alpha = -\frac{\delta}{\varepsilon}\left\{\left(\frac{d\varepsilon}{dx}\right)_\alpha - \varepsilon_x\right\} + G_1(\delta) \quad (15)$$

$$\left(\frac{d\varepsilon}{dx}\right)_\alpha = -\varepsilon G_2(\delta) \quad (16)$$

where the terms $(d\delta/dx)_\alpha$, $(d\varepsilon/dx)_\alpha$ denote differentiation along the characteristic direction, dx, $\frac{1}{2}\varepsilon\, dz$; G_1 and G_2 are the functions on the right of eqs. (9b) and (14). This system clearly breaks down if ε is zero along $z = 0$; in fact this line becomes a characteristic. In short, the above discussion shows that δ and positive ε may be specified along the line $z = 0$ and that a solution up to the limiting characteristic, AB, (at least) may be found. The solution to the right of AB, as shown above, requires the prescription of δ and ε between $z = 0$ and b (where ε is zero by symmetry), along the initial line, $x = x_i$ (the leading edge in this example). The range of influence of the initial values along this line depends upon the values themselves. Especially so in the case of ε equal to zero between $z = 0$ and b along $x = x_i$ for then, as seen above by virtue of eq. (14), the characteristics remain straight and parallel to the x-axis requiring that ε be zero throughout the field or that the end-wall flow may not penetrate the blade boundary layer. Physically, there would appear to be no reason why ε should not be so specified since the flow may impinge on the blade leading edge having only an x-wise component. However, this result does not contradict the solution obtained using eqs. (14a), (15), and (16); it merely reflects the fact that the characteristics are lines $z =$ constant and the resulting boundary layer becomes entirely two-dimensional; thus the characteristic at $z = 0$ excludes the possibility of choosing δ and ε along that line and therefore any flow arriving at the corner from the end-wall is refused, that is, separation at the corner must occur.

The treatment given by Sharma and Railly (loc. cit.) is therefore only consistent with its initial assumption, namely that ε varied linearly along the leading edge, or a parallel line, between the values given at the end-walls. The above analysis reveals that the end-walls do not impose values of ε over the blade unless there is a deliberately imposed initial condition of ε non-zero and even then the influence of the end-walls is confined to a restricted region.

The above discussion is strictly valid for the parabolic situation which occurs only at rotation numbers $-0{\cdot}04$ and $+0{\cdot}12$ (for $n = 7$) as pointed out above. For values, respectively, less than and greater than these, the equations become hyperbolic with a slight angle between the characteristics (because of the very small value of Δ in eq. (12). Nevertheless it does seem reasonable that the above findings should be regarded as generally valid. For the range of rotation numbers between $-0{\cdot}04$ and $0{\cdot}12$ the equations are very weakly elliptic which implies that the boundary conditions along $z = 0$ will always affect the solution but very weakly. If the mainstream flow is strongly accelerated then the coefficient of ε on the right of eq. (14) may become positive. In that case, ε would increase with z as the flow curved towards the end-wall and the entire field would be predictable from the line $x = x_i$ but only provided that ε is not initially zero.

CONCLUSIONS

The conclusion is drawn therefore, that strict application of boundary layer theory, namely, that boundary layers remain thin and not able to affect the free-stream, leads to the conclusion in the above case that the end-wall flow cannot affect the blade boundary layer if the boundary layer is initially two-dimensional. On the other hand, since the end-wall boundary layer develops cross-flow components (by virtue of flow curvature and Coriolis effects) therefore the above conclusion represents, at the appropriate corner, a contradiction which virtually is a requirement for corner separation. The only satisfactory method of dealing with this situation is by departing from the rigorous condition of 'thin boundary layers' by allowing interaction of the end-wall boundary layer flow with the free-stream (in particular, through the mechanism of secondary flow). The Authors are hoping to present a study along these lines in a later work.

The actual numerical solution of a problem, as the above discussion has shown, requires the specification (in the general case in relation to the present geometry) of both δ and ε from the corner point, $(x_i, 0)$, along the z-axis to $z = b$, where ε is zero, and up the x-axis as far as is necessary. It is not clear how such boundary values may be arrived at, for, as eq. (1) demonstrates, the corner-flow hypothesis only specifies the product of δ and ε and therefore an infinite range of solutions appears to be possible. The only other possibility is that the condition at the corner is changed to one of continuity of both δ and ε there and that, in order to initiate a numerical calculation, a linear variation of ε be taken between the corner value and the zero value at the centre along the initial line.

It must be recognized, however, that this latter assumption is difficult to justify, as pointed out above, when the initial flow is radial; the conclusion drawn above must therefore stand.

ACKNOWLEDGEMENTS

The Authors wish to acknowledge the support of the Science Research Council and the University of Birmingham. They also wish to thank Professor T. H. R. Skyrme for valuable discussions.

REFERENCES

(1) MOORE, J. 'A Wake and Eddy in a Rotating Radial-Flow Passage Pt. 2 Flow Model', *Trans. Amer. Soc. mech. Engrs* 1975 **95**, Ser. A, No. 3, 337
(2) SHARMA, O. P. and RAILLY, J. W. 'Coriolis, Curvature and End-wall Effects on the Boundary Layer in a Two-Dimensional Radial Impeller', University of Birmingham, Mechanical Engineering Department, Report 158, presented at 11th Israel Conference Mech. Engng., July 1977
(3) EKEROL, H. 'Effect of End-Wall Boundary Layers on the Flow in a Two-Dimensional Radial Impeller', Ph.D. Thesis, University of Birmingham, 1978
(4) COURANT, R. and FRIEDRICHS, K. O. 'Supersonic Flow and Shock Waves', Chap. 2, Interscience, 1948
(5) SKYRME, T. H. R. Personal communication, 1978

APPENDIX

The equations of motion in the context of the boundary layer over a rotating flat plate, see Fig. 2, are

$$u\frac{\partial u}{\partial x}+v\frac{\partial u}{\partial y}+w\frac{\partial u}{\partial z}-2\Omega v=-\frac{1}{\rho}\frac{\partial p}{\partial x}+\frac{\partial \tau_{yx}}{\partial y}$$

$$2\Omega u=-\frac{1}{\rho}\frac{\partial p}{\partial y} \qquad \text{(A.1)}$$

$$u\frac{\partial w}{\partial x}+v\frac{\partial w}{\partial y}+w\frac{\partial w}{\partial z}=\frac{\partial \tau_{y,z}}{\partial y}$$

It may be shown that

$$-\frac{1}{\rho}\frac{\partial p}{\partial x}=U_1U_1'-2\Omega\int_y^\delta\frac{\partial u}{\partial x}\,\mathrm{d}y-2\Omega U_1\frac{\mathrm{d}\delta}{\mathrm{d}x} \qquad \text{(A.2)}$$

Eliminating v with the aid of the equation of continuity then the equation of the boundary layer becomes

$$u\frac{\partial u}{\partial x}-\frac{\partial u}{\partial y}\int_0^y\frac{\partial u}{\partial x}\,\mathrm{d}y-\frac{\partial u}{\partial y}\int_0^y\frac{\partial w}{\partial z}\,\mathrm{d}y-U_1U_1'+w\frac{\partial u}{\partial z}$$

$$=\frac{1}{\rho}\frac{\partial \tau_{yx}}{\partial y}$$

$$+2\Omega\left\{-\int_0^y\frac{\partial u}{\partial x}\,\mathrm{d}y-\int_0^y\frac{\partial w}{\partial z}\,\mathrm{d}y-\int_y^\delta\frac{\partial u}{\partial x}\,\mathrm{d}y-U_1U_1'\right\} \qquad \text{(A.3)}$$

$$u\frac{\partial w}{\partial x}-\frac{\partial w}{\partial y}\int_0^y\frac{\partial w}{\partial x}\,\mathrm{d}y-\frac{\partial w}{\partial y}\int_0^y\frac{\partial w}{\partial z}\,\mathrm{d}y+w\frac{\partial w}{\partial z}=\frac{1}{\rho}\frac{\partial \tau_{yz}}{\partial y} \qquad \text{(A.4)}$$

Integration of these equations over thickness δ gives eqs. (3) and (4).